

https://doi.org/10.70917/jcc-2025-014 Article

Solar PV Powered Cooling with Thermal Energy Storage for Rural Healthcare Facilities in Malaysia

Amirudin Abdullah ¹, Hasila Jarimi ^{1,2,*}, Tianhong Zheng ², Yanan Zhang ², Tajul Rosli Razak ^{2,3}, Emy Zairah Ahmad ⁴, Ubaidah Syafiq ¹, Ahmad Fazlizan ¹, Norasikin Ahmad Ludin ¹, Noor Muhamad Abd. Rahman ⁵, Mohd Haikal Jamaludin ⁵ and Saffa Riffat ²

- Solar Energy Research Institute, Universiti Kebangsaan Malaysia, Bangi 43600, Selangor, Malaysia
- ² Department of Architecture and Built Environment, The University of Nottingham, University Park, Nottingham NG7 2RD, UK
- ³ Faculty of Computer and Mathematical Sciences, Universiti Teknologi MARA, Shah Alam 40450, Selangor, Malaysia
- ⁴ Faculty of Electrical Technology and Engineering, Universiti Teknikal Malaysia Melaka, Hang Tuah Jaya, Durian Tunggal 76100, Melaka, Malaysia
- ⁵ Engineering Services Division, Ministry of Health Malaysia, Putrajaya 62590, Malaysia
- * Correspondence author: Hasila.jarimi@ukm.edu.my

Abstract: This paper presents an analysis of an off-grid solar cooling system designed for rural healthcare facilities in Malaysia, where the electricity infrastructure is often unreliable, affecting the delivery of essential healthcare services. Aiming to minimize the reliance on electrical battery storage, the system utilizes a DC-powered vapor compression cooling unit directly driven by photovoltaic (PV) solar panels with energy storage using thermal energy storage. Meanwhile, electrical battery storage was designed sufficiently for auxiliary electrical equipment. In addition, the system was designed to maintain indoor air temperatures within a comfortable range as per MS 1525–2014 and DOSH 2010 standard. In conducting the feasibility study of the proposed idea, we have designed and installed a 5-kW cooling system at a test room facility in Malaysia. The performance of the system was monitored over various conditions, and the results show that indoor temperatures were kept between 22 °C to 26 °C, even when external temperatures reached 35 °C. Additionally, levelized cost of cooling analysis, and a simple payback period indicates that cost per kWh of cooling is only 0.033 USD and less than 2 years respectively. This feasibility study not only demonstrates the technical viability of solar-powered cooling in rural healthcare settings but also highlights its potential for broader application in similar off-grid regions, contributing to sustainable energy solutions in the healthcare sector.

Keywords: solar cooling; PCM storage; TRNSYS; photovoltaic (PV) systems

1. Introduction

Building operations account for 30% of global final energy consumption and 26% of energy-related emissions. Of these emissions, 8% are direct emissions from buildings, while 18% are linked to the production of electricity and heat used within buildings. In 2022, energy consumption for space cooling increased by over 5% compared to 2021. This growing demand for cooling significantly impacts peak electricity loads, particularly on hot days, potentially leading to power outages (International Energy Agency, n.d.). Conventional air-conditioning systems typically rely on electrically driven AC vapor compression cycles powered by fossil fuels, which contribute substantially to CO₂ emissions and exacerbate global warming. Solar cooling technologies offer a sustainable alternative by converting solar energy into cooling through two main mechanisms: solar photoelectric conversion and solar thermal conversion (Gao et al., 2018). In photoelectric conversion, photovoltaic (PV) cells transform solar energy



Copyright: © 2025 by the authors

into electricity to power conventional vapor-compression chillers, which may be DC- or AC-powered. In contrast, solar thermal conversion uses solar collectors to convert solar energy into thermal energy, which drives cooling systems such as absorption, adsorption, and desiccant cooling. Among these, solar absorption cooling is the most common, considered cost-effective and widely available (Gao et al., 2018). However, compared to solar absorption systems, solar PV refrigeration systems are simpler in design and easier to maintain (Gao et al., 2021). Recent studies show that in some regions, the economic performance of PV cooling systems can surpass that of solar thermal systems due to declining PV panel costs (Ayadi & Al-Dahidi, 2019). Despite their potential, direct PV-powered compressors cannot operate during nighttime or low solar irradiance, highlighting the need for energy storage. Moreover, while solar-powered cooling systems are advancing, they still face significant limitations, particularly in rural areas. Issues such as affordability, ease of use, and reliability under fluctuating solar conditions remain critical, especially in rural healthcare settings, where continuous cooling is essential for patient comfort and preserving medical supplies.

In off-grid PV cooling systems, batteries are often used to store energy, but they increase both costs and risk of accidents. As a result, researchers are exploring ways to reduce battery usage in these systems (Gao et al., 2021). For larger PV refrigeration systems, battery costs remain high, and frequent replacements due to degradation increase both investment and operational costs, while raising environmental concerns at the end of their lifecycle. Consequently, integrating thermal storage with PV-powered vapor compression systems has gained significant attention in recent years. Several studies have explored the use of ice thermal storage in refrigeration and air-conditioning systems. A system using ice thermal storage and battery storage with an AC compressor demonstrated, through theoretical calculations and experimental testing, that it could stably serve users for 4 hours at night. However, the refrigerator's ice-making efficiency was only 50.19%, leading to low energy efficiency (Xu et al., 2017). Another study on a refrigerated warehouse system using a DC variable frequency compressor with different PV capacities showed that increasing the PV capacity-to-compressor ratio by 10% reduced solar intensity requirements and shortened the temperature reduction time by 32 minutes (Liang et al., 2022).

For a 3HP household air conditioning system with ice thermal storage and a single coil cold storage, experimental results revealed that a refrigerator powered by the grid had a coefficient of performance (COP) 6.31% higher than one powered by distributed PV energy. Additionally, the COP of a water chiller air conditioning system was 1.38 times higher than that of the ice storage mode (Xu & Li, 2022). In a study on semi-dynamic modelling of a PCM ice storage system with battery and AC compressor for building retrofits, it was suggested that a PCM-to-battery storage capacity ratio greater than 6 is required to achieve optimal renewable energy penetration (Varvagiannis et al., 2021). Meanwhile, experimental and theoretical work on a photovoltaic direct-driven ice storage air-conditioning system (PDISAC) showed that it could maintain room temperatures below 298.15 K for two hours at night (Han et al., 2021). Finally, a photovoltaic vapor compression system for a 50-Liter refrigerator, tested in a hot arid climate with and without PCM, proved suitable for post-harvest crop refrigeration in remote areas. It was found to achieve a COP of 1.22 and maintain a storage temperature of 5 °C by the third day and 0 °C by the sixth day (El-Bahloul et al., 2015).

Despite these advancements, conventional AC vapor compression units still face significant limitations in rural settings. These include high startup current demands, inconsistent solar radiation, and the high costs of battery storage and inverters, all of which hinder the implementation of affordable and reliable solutions. Therefore, there is a clear need for a more straightforward, more cost-effective offgrid solar cooling solution that can maintain indoor air quality and comfort while being easy to implement and affordable in rural areas. To address this gap, this research focuses on designing a DC-powered vapor compression cooling system that integrates both thermal and battery energy storage. The system is tailored specifically for rural healthcare facilities to ensure stable cooling performance under fluctuating solar conditions. The key contributions of the research are identified as follows: first is in the design of the off-grid DC vapor compression system powered by solar energy, second is on the performance evaluation in maintaining the thermal comfort of the cooled space and finally is on the economic analysis of the system in determining its feasibility in rural healthcare settings.

2. Methodology

In this study, as illustrated in Figure 1, the vapor compression cooling unit was designed with 1.9 kWp PV panel system as recommended by the manufacturer. Meanwhile, to run the auxiliary system (FCU, water pump) 660 Wp PV panel system was installed. In this research, the research methodology, as illustrated in Figure 2, was designed based on an empirical and building simulation approach. Based on validated building simulation analysis, a simulation case study was conducted which followed by a real case system installed and aimed for annual monitoring to further justify its technological readiness

level.

2.1. Experimental Design

The off-grid solar cooling system designed for this study integrates photovoltaic (PV) solar panels with a DC-powered vapor compression cooling unit and energy storage. The system consists of three main components: (1) the solar PV panels, (2) a battery bank for energy storage for the auxiliary components, and (3) a thermal storage tank. The DC vapor compression cooling unit operates directly from the energy stored in the batteries, while the thermal storage tank acts as an additional reservoir of cooling energy to ensure stable temperatures during low solar radiation periods or at night. This setup adds an extra layer of energy storage, helping to regulate indoor air temperature during periods with limited sunlight. The schematic of the experimental setup is presented in Figure 1. Meanwhile, the system components are summarized in Table 1.

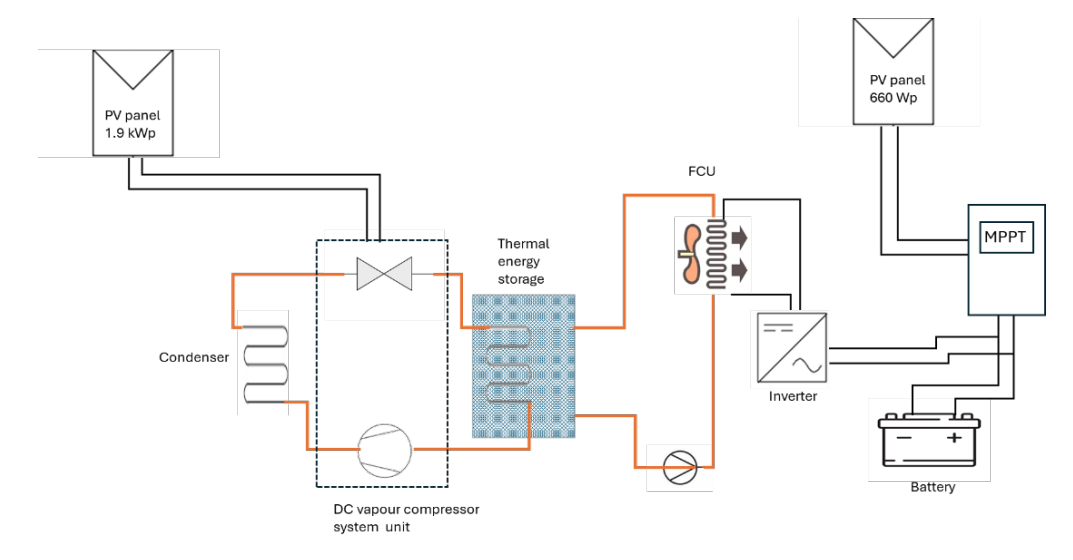


Figure 1. The schematics of the test-rig system.

Table 1. The key components and specification of the test-rig system.

Items	Specification	Quantity	
Solar PV panels	350 Wp	6 panels for DC compressor	
	Rating power at STC =350 W	2 panels for auxiliary	
	Voc = 46.2 V	components such as water	
	Isc = 9.38 A	pump and fan coil unit.	
Balance of	Electrical battery storage 12 V 200	2 units of battery	
Systems	Ah	1 unit of other components	
	MPPT solar charge controller 60		
	Amp 24V		
	Inverter at 300-Watt capacity		
Water pump	30 Watt, 24 VDC powered water		
	pump		
Fan coil unit	50-Watt BLDC motor fan at	1 unit	
	maximum of 5 kW cooling capacity		
Compressor	DC 90 v-280V, Power: 410 Watt –	1 unit	
	1920 Watt		
Refrigerant	R32		
Thermal energy	Water	300 l tank with Double coil for	
storage		water and direct cooling for	
		water	

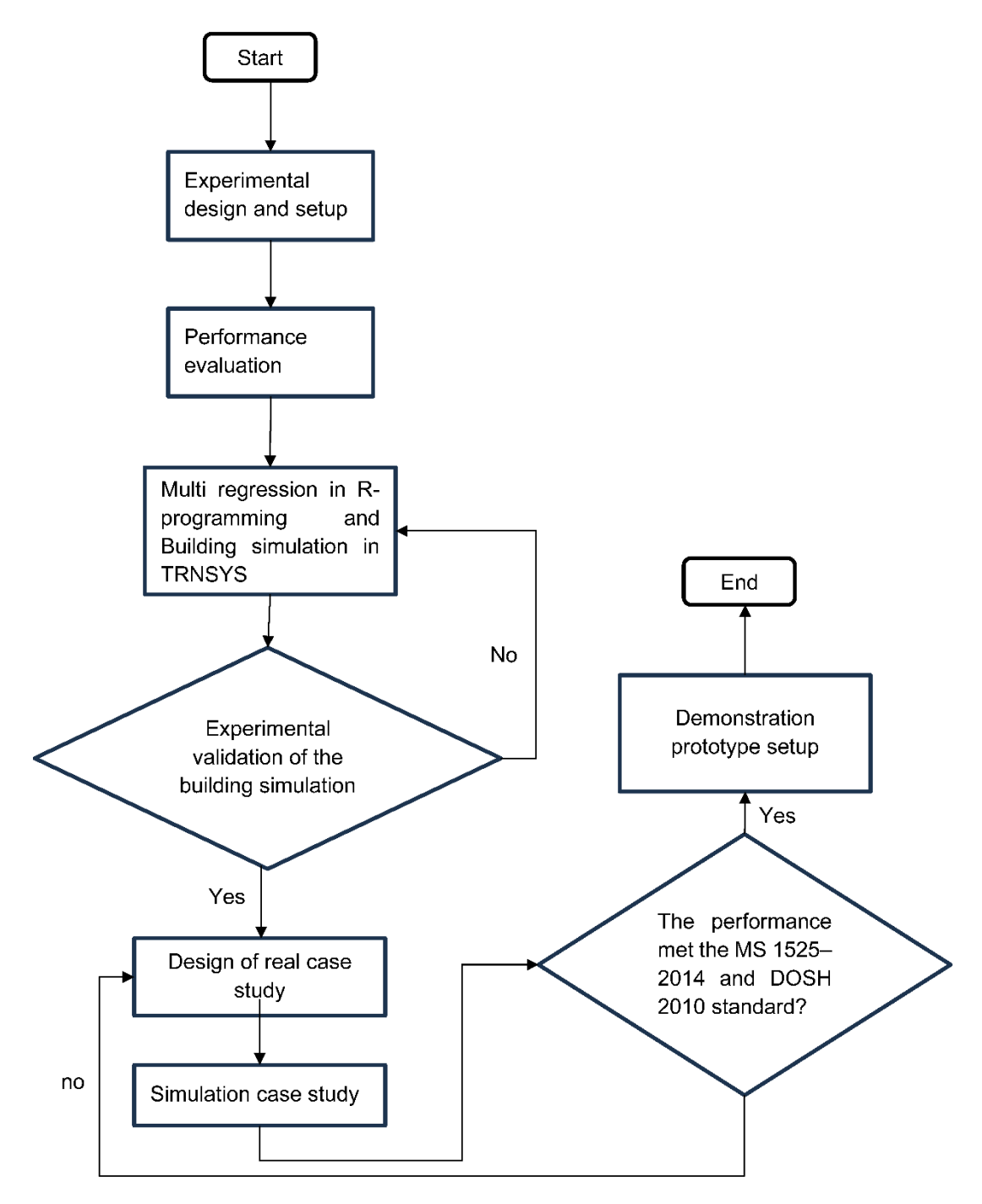


Figure 2. The framework of the research method.

2.2. Experimental Setup and Performance Parameters

The system was installed in a test room, as presented in Figure 3, designed to simulate the typical conditions of rural healthcare facilities in a tropical climate. The test room setup was configured to replicate real-world conditions in such facilities, ensuring the system's performance under typical environmental stresses. The room has a floor area of 15 square meters and was equipped with temperature and humidity sensors to monitor thermal comfort performance. External environmental conditions, such as solar radiation and ambient temperature, were also recorded throughout the experiment.

The system was tested over a period of one week, with measurements taken daily from 8:00 AM to 5:00 PM. It is worth noting that one of the limitations of lab-scale field testing is the presence of noise and variation in the collected data. With that said, the most consistent data with minimal noise and variation were selected to validate the simulation analysis, which explains the one-week testing period.

Nevertheless, the data collected is sufficient for simulation validation purposes. During the testing period, solar radiation levels were recorded using a pyranometer, and indoor air quality parameters were monitored using a multi-channel data logger. The data collected included room temperature, relative humidity, compressor power consumption, and solar radiation levels.

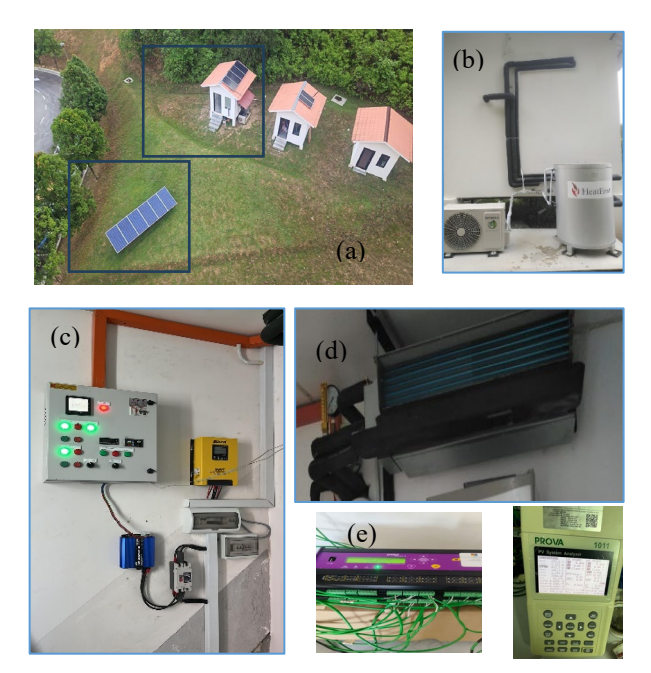


Figure 3. (a) The top view of the test-rig test setup (b) Vapor compression unit with thermal energy storage (c) PV control system (d) Fan coil unit (FCU) and (e) the data acquisition unit.

In this study the useful cold produced and stored $Q_{cooling}$, was calculated by taking into consideration of the total enthalpy of the thermal energy storage Q_{Th} , and the useful cooling energy by the working fluid Q_{FCU} given in Equation (1) where Δt is time in hour:

$$Q_{cooling} = Q_{Th} + Q_{FCU}$$

$$Q_{cooling} = \frac{m_{Th}c_{Th}(\Delta T_{Th})\Delta t}{3600} + [\dot{m}_{fan}c_{air}(T_o - T_i)]\Delta t$$
 (1)

The coefficient of performance of the system is measured by the overall useful cooling capacity of the system over the total energy input into the system regardless of the type of sources i.e. from PV or from the grid and is given by Equation (5).

$$COP_{system} = \frac{Q_{cooling}}{P_{in}}$$

$$P_{in} = Power\ input$$
(2)

Thermal comfort refers to a state of mind that expresses satisfaction with the surrounding environment, significantly influenced by both temperature and relative humidity. In healthcare facilities, keeping optimal thermal comfort is crucial not only for comfort but also for the health and safety of both patients and staff. Proper thermal conditions and good air quality can reduce stress, aid in faster recovery, and enhance the overall healthcare experience. The two are interdependent; poor air quality can diminish the perceived thermal comfort and vice versa, underscoring the importance of monitoring both aspects closely. In this study, our aim is for the room to reach acceptable ranges outlined by MS 1525–2014 and DOSH 2010: 24.0 - 26.0 °C at 50 - 70% RH and 23.0 - 26.0 °C at 40 - 70% RH respectively (Khalid et al., 2019). In terms of the economic analysis, we employed the levelized cost of cooling (LCOC,) a crucial parameter for economic evaluation, to compare with conventional system being the cooling system using grid connected AC vapor compression system without the thermal storage. The LCOC was computed using the Equation (3) as in (Behzadi et al., 2021; Louvet, n.d.).

$$LCOC = \frac{I_o + \sum_{j=1}^{n} \frac{M_j + F_j}{(1+d)^j}}{\sum_{j=1}^{n} \frac{Q_{cooling}}{(1+d)^j}}$$
(3)

 I_o , M_j and F_j in Equation (8) is the initial investment, maintenance, and fuel costs in the *j*th year respectively. Additionally, the discounted rate d in this study is taken as 8%.

2.3. Building Simulation in TRNSYS

In this study, the performance of a solar-powered cooling system was simulated using TRNSYS 18, based on the design, specifications, and location of the test-room at 2.75 m × 2.75 × 2.75 m in size. The simulation results, in terms of room temperature (Troom) and fan coil unit temperature (Tfcu_in), were validated against experimental data. Using the validated simulation model, the performance of the system can be predicted for different building types and locations by adjusting and modifying the building design parameters in TRNSYS. In this research, the design parameters of the test room were employed. Meanwhile, the output parameters for the evaporator temperature were derived from the multi regression analysis, which served as the input for the PCM storage tank unit. Additionally, it is worth emphasizing that the PCM tank was simulated, and its parameters were adjusted until the FCU temperature aligned with the experimental results.

The schematic of the TRNSYS layout is presented in Figure 4. It is important to note that the TRNSYS simulation was designed to evaluate the potential of the proposed cooling system for providing thermal comfort to the simulated area or space in a building. In this research, the DC vapor compression component was modelled as one of the elements in TRNSYS, while the off-grid PV system, which powers auxiliary components (such as the water pump and FCU), was assumed to operate consistently and was considered to have no direct impact on the overall thermal performance of the building.

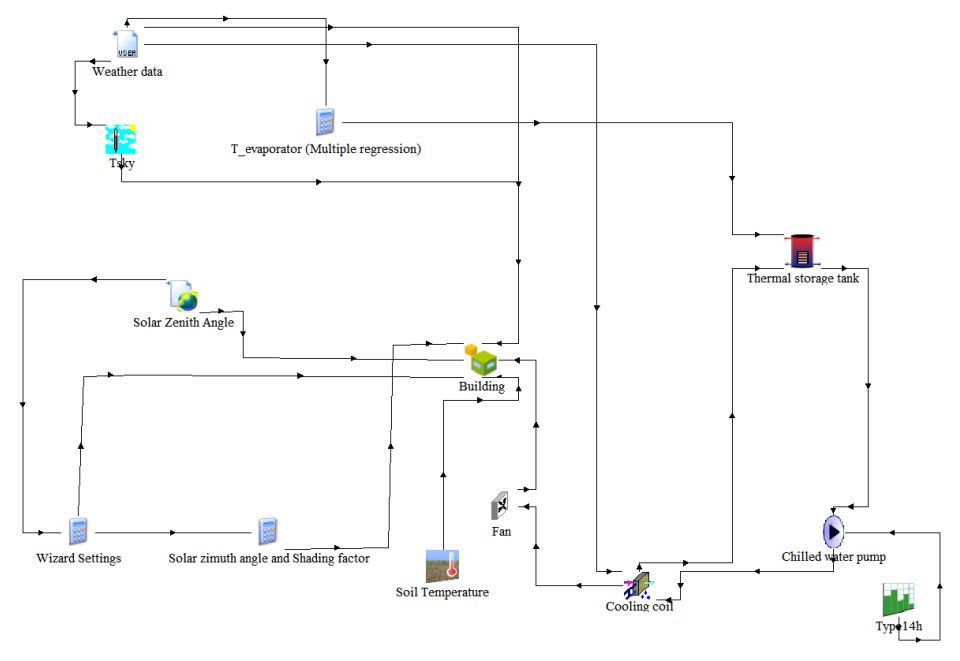


Figure 4. TRNSYS layout used in the building simulation.

3. Results and Discussions

In this section we discuss the outcomes from the experiment by taking into consideration the thermal comfort in the form of room temperature and relative humidity, the cooling capacity in comparison to the PV power generation, and finally the economic analysis of the system based on the levelized cost of cooling. In this section we discuss the simulation analysis in TRNSYS and its validation followed by a simulation case study for a selected location in rural area Malaysia.

3.1. Thermal Comfort Analysis

In analyzing the performance, we have selected a one-week data as presented in Figures 5 and 6. Figure 5(a) presents the temperature variation in the room (Troom), ambient temperature (Ta), and solar radiation (G) over the course of a week, with a specific focus on the system's operation during five active days. This system is specifically designed to provide reliable cooling for rural healthcare facilities that often operate during daytime hours. During these five operational days, the cooling system effectively maintains indoor temperatures within a comfortable range, despite significant fluctuations in both ambient temperature and solar radiation throughout the day. The room temperature remains relatively stable between 24 °C and 26 °C, even as the outdoor temperature peaks around midday. This indicates the system's ability to provide a consistent indoor climate, critical for maintaining comfort and operational efficiency in rural healthcare facilities that may not have consistent grid access. Meanwhile, Figure 5(b) provides a more detailed daily analysis of the system's performance over three days, highlighting how the system responds to fluctuating solar radiation and ambient temperature while operating during healthcare or office hours (typically 8 AM to 5 PM). The graph shows that while the ambient temperature and solar radiation rise significantly during the middle of the day, the room temperature remains relatively stable. This is crucial for healthcare facilities in rural areas, as maintaining a cool and comfortable environment is essential for the well-being of patients and staff. Also, as can be seen in Figure 5(b), the cooling system, powered by solar energy, performs optimally during peak sunlight hours, but a slight rise in room temperature towards the late afternoon suggests the impact of the insulation level of the wall of the building which influences the overall thermal gain of the test facilities. Overall, the system demonstrates its effectiveness in meeting the cooling needs in terms of the room temperature over a 5-day operational period, offering a potential of sustainable solution that eliminating reliance on grid electricity, and minimizing the reliance of electrical battery storage for application in rural areas while maintaining thermal comfort.

Meanwhile, Figure 6 illustrates the variation in relative humidity (RH) for both indoor and outdoor environments, alongside solar radiation (G) over a week. It was found that when the system was operating during daytime hours, the indoor RH levels remain relatively stable, ensuring a comfortable indoor environment for both patients and healthcare staff. Meanwhile, outdoor RH fluctuates more dramatically, particularly in the early morning and late evening, following a clear diurnal pattern with the rise and fall of solar radiation. Also, worth noting here, Table 2 complements this figure by providing detailed data on room temperature, comfort level, solar radiation (G), ambient temperature, mean radiant temperature, and relative humidity (RH) at different times of the day.

Moreover, it is worth emphasizing that, as illustrated in Figures 5 and 6, despite ambient temperatures reaching as high as 31.5 °C during the afternoon (15:00), the room temperature is maintained between 24.2 °C and 26.5 °C, ensuring a comfortable indoor environment. This consistency in temperature control is critical in rural healthcare facilities where reliable cooling is important for patient care and medical equipment functionality. The relative humidity (RH) values from the table show that the system keeps indoor RH within the comfortable range (around 57–68%), even as outdoor RH varies significantly throughout the day. As the day progresses, solar radiation peaks during midday, leading to higher ambient temperatures and outdoor RH. Despite these fluctuations, the indoor environment remains stable in both temperature and humidity, with only a slight increase in temperature and RH noted towards the late afternoon (16:30–17:00). The system continues to provide comfortable conditions, with only a slight shift to "slightly uncomfortable" around the end of the operational day, which is a minor concern that could be mitigated with extended operation or additional energy storage.

This thermal comfort analysis from a user's perspective, as summarized in Table 2, when installed at the test room facility, further highlights the potential of the system's effectiveness in maintaining a stable and comfortable indoor environment if installed in rural healthcare facilities, even during periods of high solar radiation and fluctuating outdoor conditions. The performance of the cooling system, in conjunction with the management of indoor relative humidity, highlights its suitability for rural healthcare facilities, where maintaining patient comfort and efficient system operation is crucial.

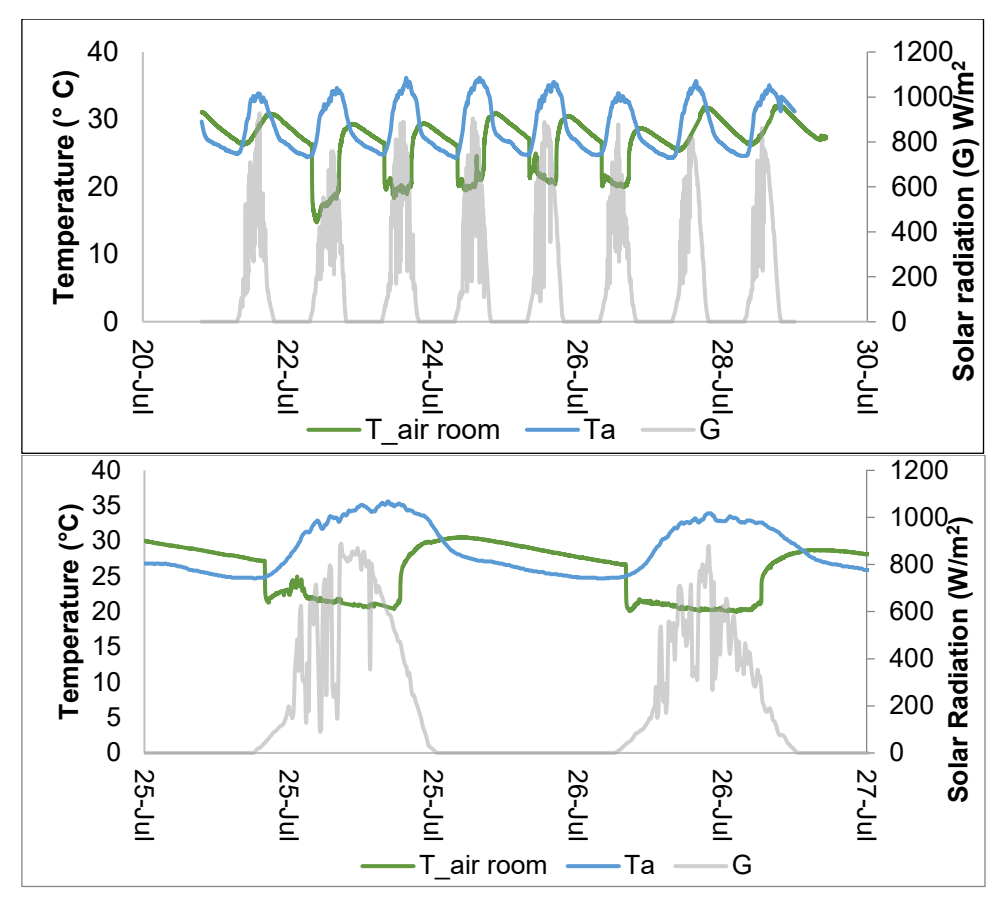


Figure 5. (a) The temperature variation in the room, ambient temperature, and solar radiation with time of day in 1 week. (b) The detailed outlook on the variation of the parameters with time of day.

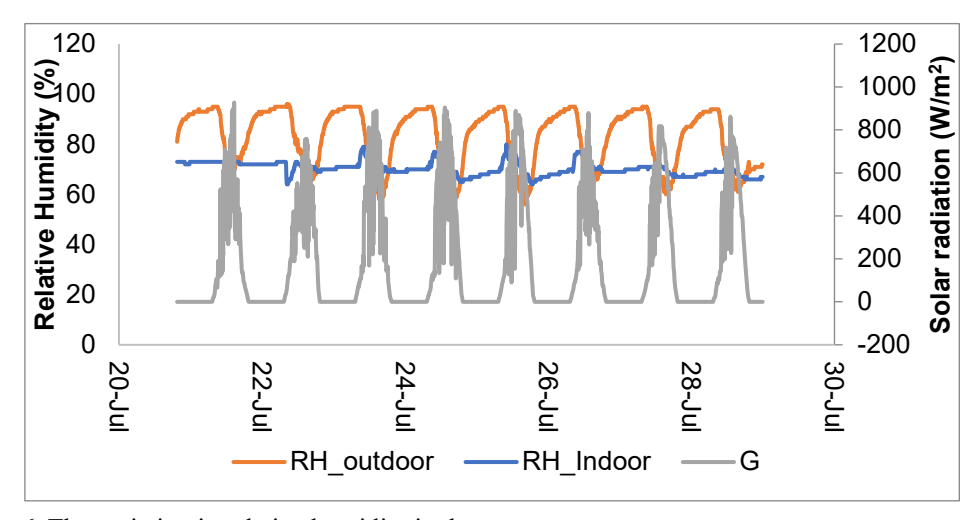


Figure 6. The variation in relative humidity in the test room.

Table 2. Thermal comfort analysis of the test room from a real user perspective in determining the comfortable level.

Time Room temperature	Comfortable level	G (W/m²)	Ambient temperature (°C)	Mean radiant temperature (°C)	RH (%)
9:30 24.7	comfortable	176	26.9	22.0	68.9
10:00 24.3	comfortable	149	26.2	20.8	63.0
10:30 24.7	comfortable	225	27.3	21.1	66.7
11:00 24.2	comfortable	780	28.8	20.4	61.2
11:3024.3	comfortable	709	28.5	20.5	60.7
12:00 24.4	comfortable	340	28.4	20.4	60.3
12:30 24.5	comfortable	793	29.5	20.5	60.0
13:00 24.9	comfortable	685	30.0	20.6	59.4
13:3025.1	comfortable	604	29.7	20.8	59.7
14:0025.6	comfortable	722	30.2	21.1	59.1
14:30 26.0	comfortable	313	30.8	21.1	58.3
15:00 26.4	comfortable	236	31.5	21.8	56.6
15:30 26.1	comfortable	313	30.8	21.6	57.2
16:00 26.2	comfortable	236	31.5	21.7	57.1
16:3026.5	slightly uncomfortable	718	30.5	22.6	57.2
17:00 26.5	slightly uncomfortable	208	29.5	22.8	57.9

3.2. Cooling Capacity Analysis

Figure 7 illustrates the variations in the cooling capacity based on the fan coil unit operation and the compressor power during five days of working hours. The system utilizes a variable-speed compressor that stores "coolth" in a thermal storage tank, enabling it to deliver consistent cooling output even as the compressor power fluctuates due to the fluctional in the available solar irradiance. Illustrated in Figure 7, peaks in cooling capacity are as high as 5 kW. However, at this cooling capacity, the compressor power rises to only around 0.8 kW due to low solar irradiance available, showing that despite the variable compressor power, the cooling capacity remains stable and reliable. This demonstrates the system's ability to provide consistent cooling while optimizing compressor operation through the use of thermal storage. Also, this implies that the stored cooling in the tank allows the system to meet cooling demand without requiring continuous high power from the compressor, which improves energy efficiency.

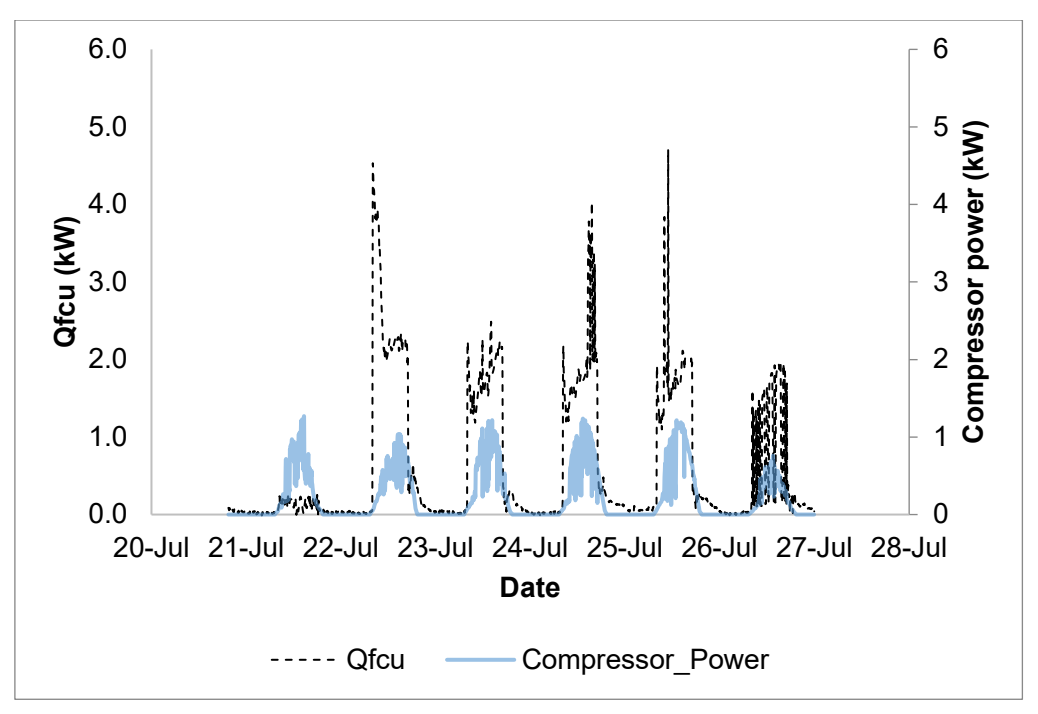


Figure 7. The variations in the useful cooling capacity provided by the FCU and the compressor power at different days of the week.

Figure 8 illustrates the performance of the system based on its coefficient of performance COP, cooling capacity and the compressor power. From the analysis, the average COP of the system was found to be approximately 3.36 with the power produced is fully from the PV panel. Also, the cooling system's performance from July 21st to July 26th is significantly affected by the input power from the photovoltaic (PV) panels, which supply 100% of the energy required by the compressor. During periods of strong sunlight, the compressor can operate at full capacity, enabling the system to provide efficient cooling and even store excess energy in the Phase Change Material (PCM) tank. This is reflected in the COP, which reaches its peak—above 5—on July 21st, when PV input is at its highest. However, as the week progresses, the COP steadily declines, falling below 2 by July 23rd and stabilizing around 2-3 for the remainder of the week. This drop in COP is attributed to either fluctuations in solar energy input or the reduced capacity in the cooling available from the PCM storage tank. As a result, system efficiency decreases, leading to a lower COP as the compressor struggles to meet real-time cooling demands with less available solar energy. Nevertheless, since the system is fully powered by PV panels, it benefits from significant energy savings by reducing reliance on grid electricity. The energy savings can be estimated by calculating the total energy consumption of the compressor and comparing it with what would have been consumed if the system had drawn energy from the grid or from the diesel powered genset. Meanwhile, during periods of high solar input, the system is able to store surplus cooling energy in the PCM tank when the room temperature is sufficiently low. This stored energy can be used later, during the night or on cloudy days when solar input is limited, allowing the system to continue providing cooling without relying entirely on real-time compressor power. However, when PV input decreases, the system cannot store enough cooling energy, and the compressor must operate continuously to meet immediate demand, which results in a lower COP.

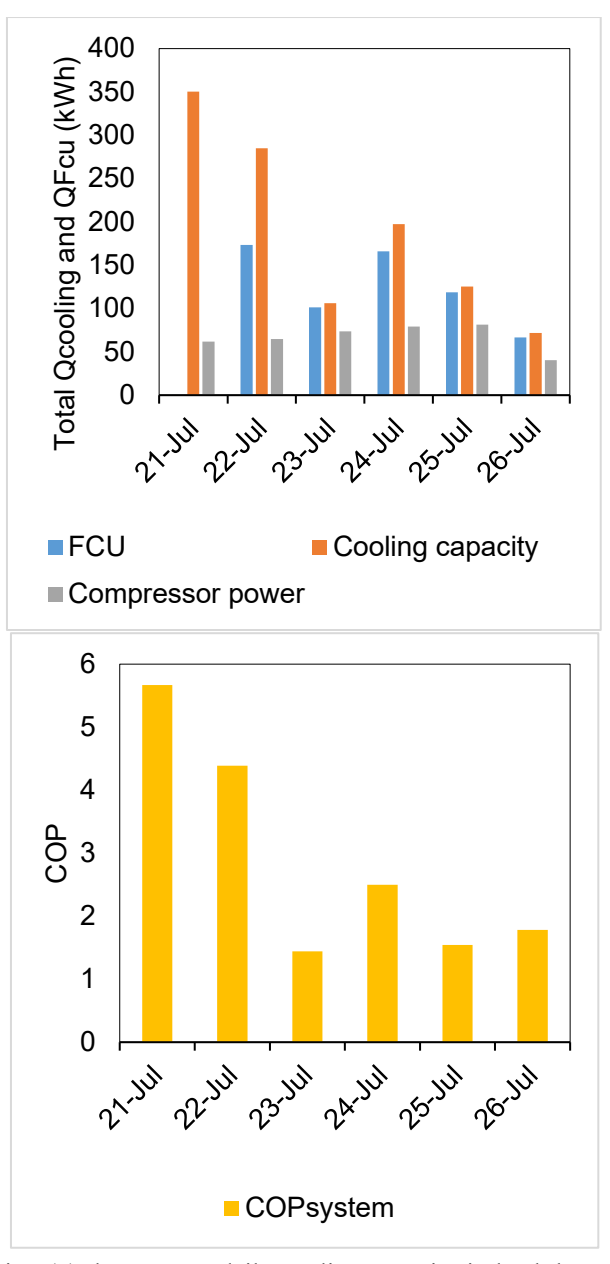


Figure 8. Graphs showing (a) the average daily cooling capacity in kWh by taking into consideration both FCU and PCM storage, and the power consumed by the compressor and (b) the average COP of the system.

3.3. Economic Analysis

From the analysis illustrated in Table 3, the total installation cost of the solar-powered air conditioning system is approximately USD 2,150, with annual operating costs of USD 215 (assumption of 10% yearly maintenance rate), leading to a total Year 1 cost of USD 2,365. In comparison to a conventional diesel-powered cooling system, the proposed solution offers annual savings of approximately USD 1,895 by eliminating the fuel costs associated with running a 5-kW air conditioning system on a genset in rural areas. This estimate assumes 8 hours of daily operation, with diesel consumption of 1 Liter per hour. Based on these savings, the system achieves a payback period of approximately 1.94 years, meaning the initial investment would be fully recovered shortly after the second year of operation. Beyond this point, the system continues to deliver long-term economic benefits, particularly valuable in remote areas where access to grid electricity is limited or unreliable.

Table 3. The estimated cost for each of the system components.

Items	Specification	Quantity	Cost (USD)
Solar PV panels	350 Wp	6 panels for DC	725
	Rating power at STC $=350$	compressor	
	W	2 panels for auxiliary	
	Voc = 46.2 V	components such as	
	Isc = 9.38 A	water pump and fan coil unit.	
Balance of	Electrical battery storage 12	2 units of battery	475
Systems	V 200 Ah	1 unit of other	
	MPPT solar charge controller 60 Amp 24V Inverter at 300-Watt	components	
	capacity		• • •
Water pump	30 Watt, 24 VDC powered water pump		250
Fan coil unit	50-Watt BLDC motor fan at maximum of 5 kW cooling capacity	1 unit	
Compressor	DC 90 v-280V, Power: 410 Watt – 1920 Watt	1 unit	600
Refrigerant	R32		
Thermal battery	Water	300 l tank with Double coil for water and direct cooling for water	100
Total cost		cooming for water	2,150

Moreover, the system significantly contributes to environmental sustainability. Over its 20-year operational life, with a discount rate of 8% and no battery replacement costs, the Levelized Cost of Cooling (LCOC) is calculated to be approximately USD 0.033 per kWh. This reflects the low average cost of cooling provided by the system over its lifetime. In addition to reducing operational costs, the system decreases reliance on diesel fuel, which is a common energy source in rural communities, and substantially cuts carbon emissions, offering a viable and environmentally responsible solution for offgrid cooling needs.

3.4. Multi Regression in R-Programming

Due to the complex relationship between the ambient parameters and the performance of the vapor compression unit, multiple regression analysis is used to correlate the evaporator temperature of the vapor compression unit (Tevap) with the independent variables, ambient temperature (Ta) and solar irradiance (G). By analyzing multiple predictors simultaneously, multiple regression enhances the reliability of predictions and supports informed decision-making. R is a powerful tool for regression modelling, offering comprehensive capabilities through its base functions and extensive package ecosystem. The lm() function, part of R's core stats package, is the backbone for constructing multiple regression models. R's emphasis on reproducibility and flexibility makes it a preferred choice for researchers and practitioners, enabling continuous statistical analysis and programming integration. In this study, the R code implements a multiple regression model using the lm() function to analyze the relationship between the dependent variable which is the evaporator temperature of the vapor compression unit (Tevap) and the independent variables ambient temperature (Ta) and solar irradiance (G), as shown in Figure 9. First, the dataset is read with the read excel() function and relevant variables are selected for analysis. The model is built using the lm() function, which defines how Tevap depends on Ta and G. The model's coefficients, including the intercept and slopes, are then extracted and printed for further interpretation. While the code does not explicitly perform predictions, the coefficients allow for manual or programmatic prediction of "Tevap" based on new values of "Ta" and "G", offering insights into how these predictors influence the outcome.

```
| Source on Save | Source on Save | Source on Save | Source of Source on Save | Source on S
```

Figure 9. Multivariable regression in R-programming to correlate between the evaporator temperature (Tevap) with ambient temperature Ta and solar irradiance (G).

As can be seen in Figure 10, the regression model results provide the estimated coefficients that describe the relationship between the dependent variable, "Tevap", and the independent variables, "Ta" and "G". The intercept value of 8.30612 represents the predicted value of "Tevap" when both "Ta" and "G" are zero, serving as the model's baseline. The coefficient for "Ta" is 0.44543, indicating that for every one-unit increase in "Ta", "Tevap" increases by approximately 0.44543 units, assuming "G" remains constant, reflecting a positive relationship. Conversely, the coefficient for "G" is -0.03319, suggesting that for each one-unit increase in "G", "Tevap" decreases by about 0.03319 units, assuming "Ta" remains constant, signifying a weak negative relationship.

```
Call:
lm(formula = Tevap ~ Ta + G, data = input)

Coefficients:
(Intercept) Ta G
8.30612 0.44543 -0.03319
```

Figure 10. Result of the multiple regression.

3.5. Building Simulation Analysis in TRNSYS

Figure 11(a) illustrates the comparison between the simulated and experimental values for the air outlet temperature of the fan coil unit (Tfcu in) over the period from July 21 to July 27. The plot reveals a similar fluctuation pattern between the two datasets, indicating that the simulation model aligns with the general trend of temperature changes observed experimentally. However, there are some noticeable deviations, particularly in the peak and trough regions during the first two days of operation. The experimental data displays sharper declines at certain points, whereas the simulation data follows a smoother trend, with lower FCU temperatures obtained experimentally. These inconsistencies could be attributed to external factors in the real-world experiment that were not accounted for in the simulation model, such as transient variations in ambient conditions or specific operational cycles of the equipment, especially since the temperature of the FCU is highly dependent on the volumetric flow rate of the air supply. Meanwhile, Figure 11(b) presents the comparison of room temperature (Troom) between experimental and simulated values for the mean room temperature over the same period. Here, the simulated and experimental data for room temperature exhibit a high degree of alignment, with both lines closely following each other throughout the entire timeframe. Minimal deviations are observed, indicating that the simulation model is highly effective at capturing the dynamics of room temperature changes. This strong correlation also suggests that the model is reliable for predicting room temperature, which may be a critical parameter in the study. The correlation was further supported by error analysis using the Mean Absolute Error (MAE), which shows deviations of 6.41 °C and 2.71 °C for Tfcu in and Troom, respectively. As expected, the MAE for Tfcu in is higher due to the aforementioned variations in the real-world experiment.

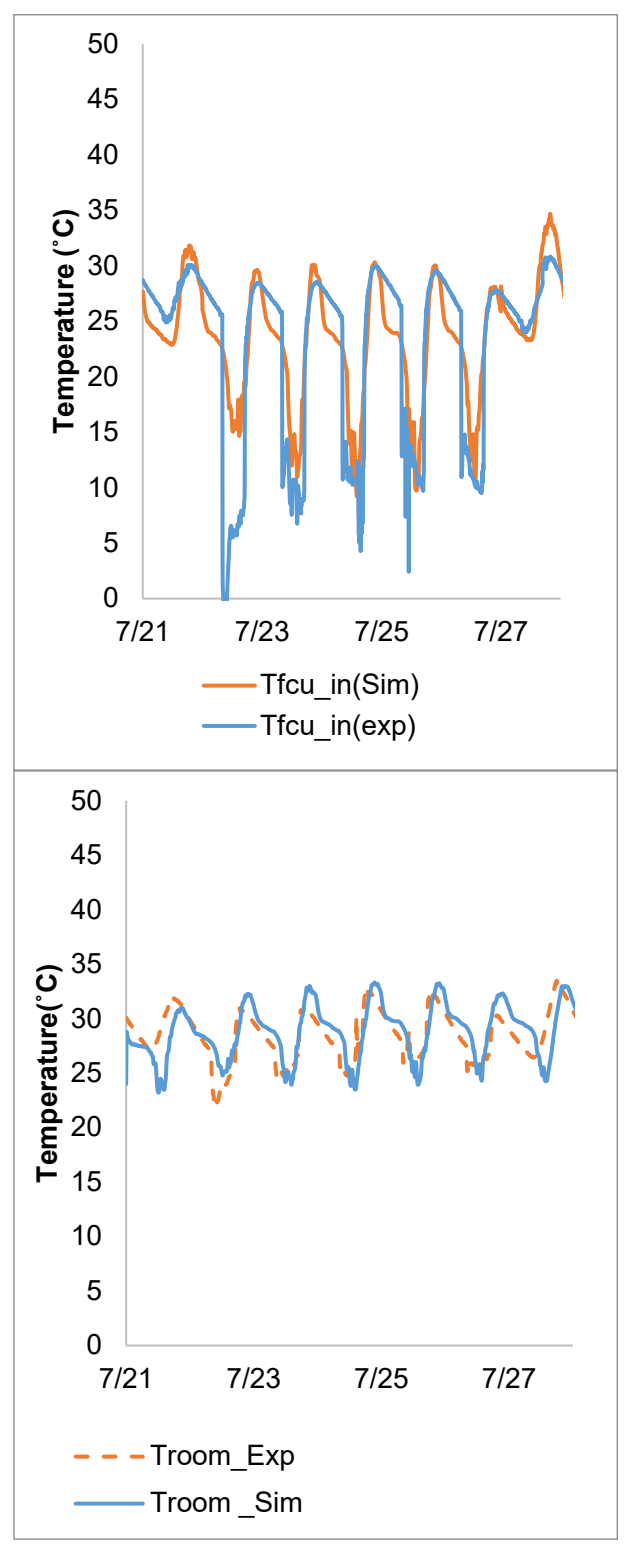


Figure 11. The comparison between simulation and experimental data.

3.6. Simulation Case Study

The hemodialysis center in Pahang, Malaysia, at coordinates of 3.9146° N, 103.0327° E, was selected as a simulation case study location. To conduct the simulation, the size of the room that was simulated is based on the plan as shown in Figure 12. The area that is aimed to be covered by the cooling is system is at $9.3~\text{m}\times6.0~\text{m}$. The building simulation was performed in TRNSYS. By inputting the building

parameters, the FCU specifications obtained from the multiple regression equation previously discussed in R-programming, and climate data such as ambient temperature and solar radiation, we simulate how the building responds to different environmental and operational conditions, which allows us to have an overall performance of the cooling system. In this study, we particularly give our focus on the room temperature and relative humidity of the area aimed to be cooled.

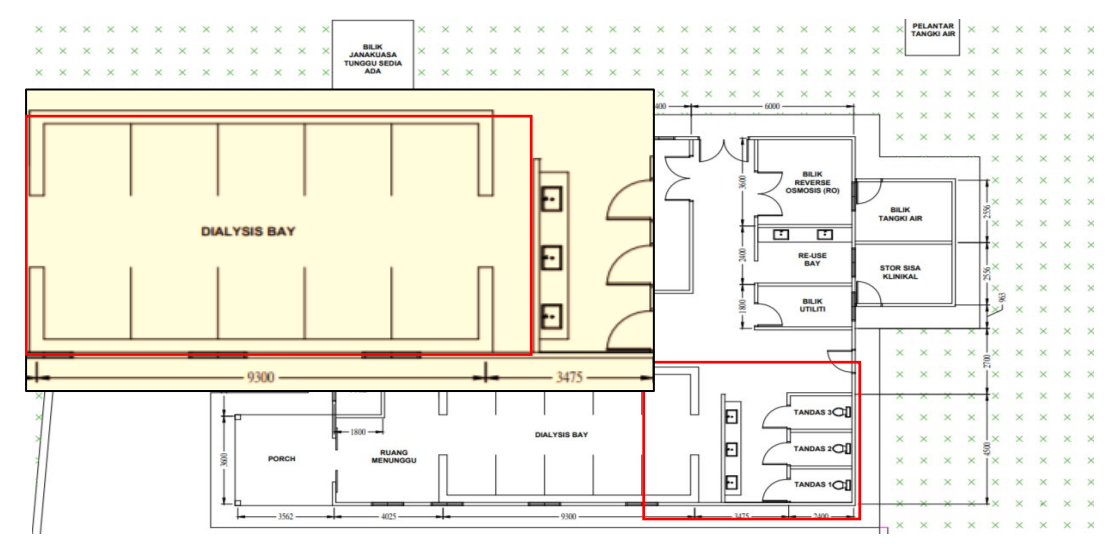


Figure 12. The drawing plan of the cooling space.

The time-series plot in Figure 13 shows the simulated data for the building case study, illustrating the interaction between indoor and outdoor environmental parameters, including room relative humidity (RHroom), room temperature (Troom), ambient temperature (Ta), and solar irradiance (G) over a defined period of day and night cycles. This simulation provides an in-depth look at how the building environment responds to external conditions, and it gives an explanation of the effects of solar irradiance on indoor climate control variables. The solar irradiance (G), follows a typical diurnal pattern, peaking around midday and falling to zero overnight. During the daytime, as irradiance rises, an increase in both indoor and ambient temperatures can be observed, which is common in buildings exposed to solar radiation. The room temperature (Troom) and ambient temperature (Ta) indicate relatively stable trends, with some variations across the day. In addition, the room temperature demonstrates a more regulated profile compared to ambient temperature, likely due to the effects of building insulation, thermal mass, and the cooling system working to maintain comfortable indoor conditions.

It is crucial to note that the cooling system was set to operate during working hours (8 am to 5 pm). Within this duration Figure 13 indicates that the room temperature varies between 24–26 °C, which falls within the thermal comfort level of a building. Meanwhile, the simulation shows that the room relative humidity (RHroom), displays an inverse relationship with both temperature and irradiance. As the temperature rises during the day, the relative humidity tends to decrease, likely due to the operation of the FCU and natural air-drying effects as temperatures increase. Also, similar to the room temperature, the relative humidity values also fall within the thermal comfort level as stated by MS 1525–2014.

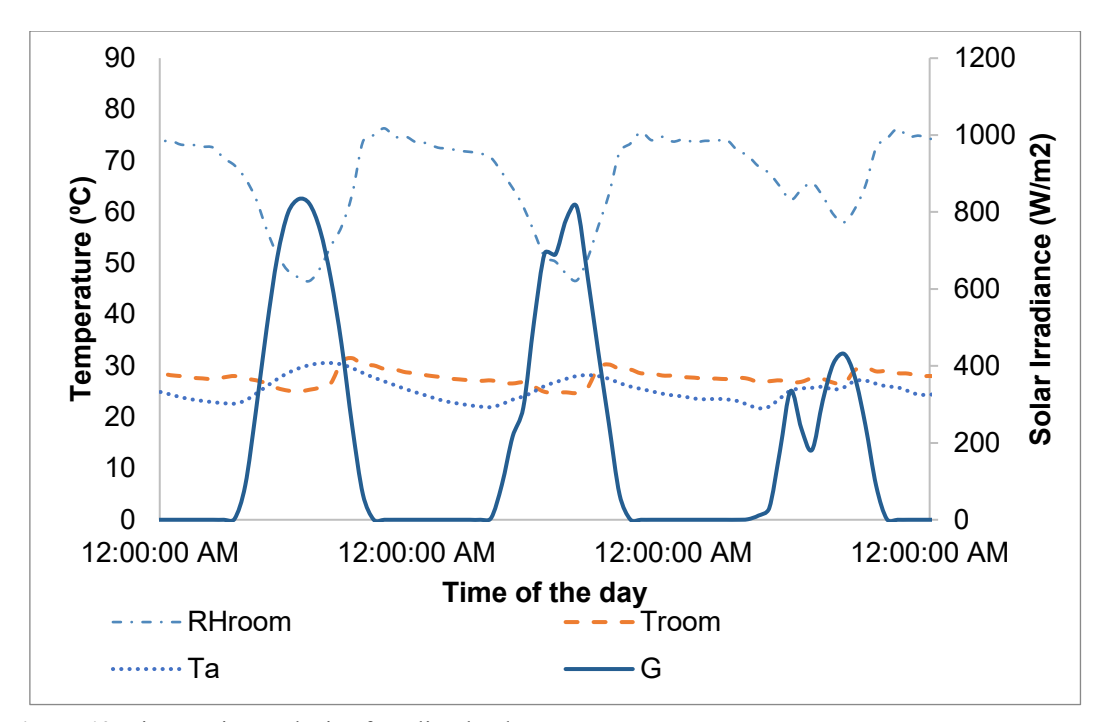


Figure 13. Time-series analysis of cooling load.

Figure 14 presents a time-series analysis of cooling load (Qcooling) and photovoltaic (PV) power production, measured in watts, over a multi-day period, with distinct peaks and troughs aligning with the daily fluctuations in solar irradiance and ambient temperature. The cooling load displays a characteristic increase during daylight hours, reaching its peak around midday when external temperatures and solar heat gains are at their highest. This pattern reflects the increased demand for the cooling system to maintain indoor thermal comfort as solar radiation and ambient temperatures rise. A crucial point to note is that the PV power production is lower compared to the cooling demand/capacity, implying a COP of more than 1. Also, even at peak period (during the day), the cooling demand can still be met, owing to the excess cooling energy that has been stored during the day. Based on the analysis, we confirm that the system can be set up for a real-scale application as illustrated in Figure 15, for a real case study at the selected location. The outcomes are expected to be discussed in a technical report expected to be published at the end of next year.

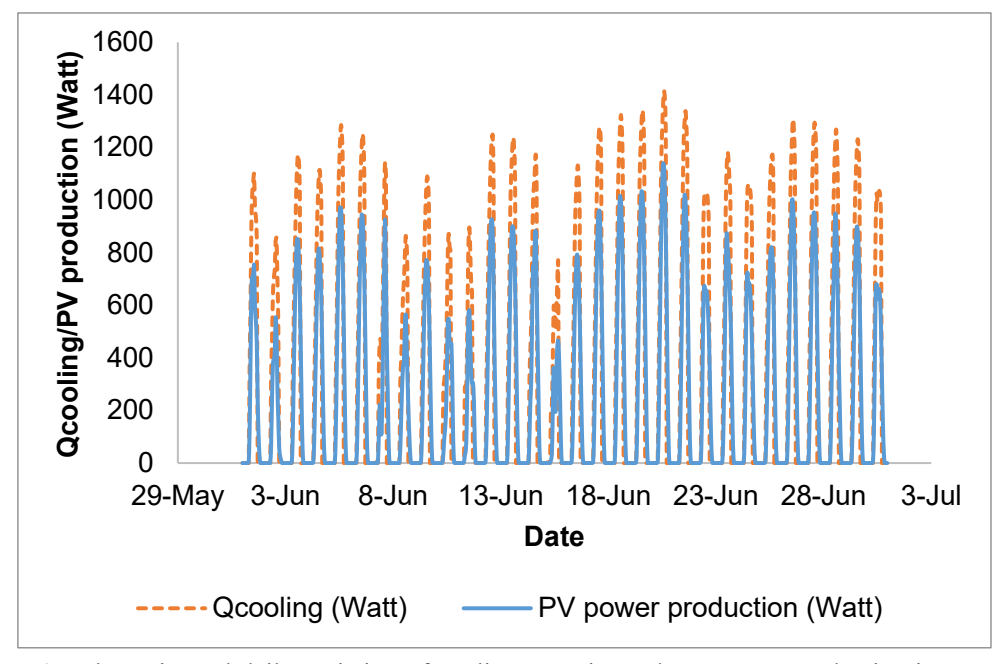


Figure 14. The estimated daily variation of cooling capacity and PV power production in one month period.



Figure 15. Real case study installation at a rural healthcare facility in Malaysia (a) Shows the installed solar PV panel system (b) PCM storage attached to the vapor compression unit and (c) the balance of system for the solar powered cooling system.

While the outcomes of the system are not yet comprehensive and ready for detailed discussion, from an installation perspective, the scalability of the system is seen feasible due to the following justifications:

- The materials used primarily locally available to manufacture the thermal storage tank and easy to move.
- 2. Logistically, each of the components can be separated and transferred in smaller components which made it possible for rural installation.
- 3. Additionally, unlike electrical battery storage, which has a shorter lifespan, we intend to use phase change materials that have a longer lifetime, low-cost and are easy to obtain. This has been justified from the levelized cost of cooling analysis discussed in Section 3.3.

4. Conclusions

Thermal comfort in healthcare facilities, particularly in rural areas with limited electricity access, is critical but often overlooked. As global temperatures rise due to climate change, addressing heat stress and its impact on human health becomes even more urgent. Ensuring equitable access to affordable cooling systems for underserved regions is a complex challenge that must be addressed through innovative solutions. This study investigates a fully solar-powered cooling system designed to improve thermal comfort in these areas. The system significantly reduces reliance on electrical battery storage by 80%, lowering both capital and maintenance costs over its lifespan. While the system has demonstrated reliability in terms of performance and economics, its scalability remains a critical consideration for wider adoption. Through empirical modelling and TRNSYS building simulations, the system's potential for rural implementation was explored. A prototype installation at a selected location is currently being monitored, with results expected within six months. These findings will provide valuable insights into the commercial feasibility of solar-powered cooling systems for rural healthcare facilities. This research contributes to the growing body of knowledge on sustainable cooling solutions and offers a reference point for further optimization and real-scale applications, including the potential health benefits of reducing heat stress in vulnerable populations.

Author contribution statement

Amirudin Abdullah: Review & Editing, Investigation, Methodology, Experiment. Hasila Jarimi:Funding, Supervision, Writing original article, Investigation, Methodology, TRNSYS. Tianhong Zheng and Zhang Yanan: Review & Editing, Methodology (Experiment). James Riffat: Review & Editing. Tajul Rosli Razak: Review & Editing, Methodology (Prediction modelling in R programming). Emy Zairah: Funding, Review & Editing, Investigation, Validation. Ubaidah Syafiq, Ahmad Fazlizan: Supervision, Methodology. Norasikin Ahmad Ludin, Noor Muhamad Abd. Rahman, Mohd Haikal Jamaludin: Funding, Supervision and Methodology. Kamaruzzaman

Sopian: Funding and supervision. Saffa Riffat: Original idea, and Funding. All authors have read and agreed to the published version of the manuscript.

Acknowledgements

We would like to acknowledge UEM Edgenta SDN BHD and Royal Society (ICA\R1\201236) for the financial support for this research. Besides, we would like to acknowledge Universiti Kebangsaan Malaysia (RS 2024_006) and (RS 2020-006). The main author, Dr. Hasila Jarimi, would also like to thank UKRI for the Marie Skłodowska-Curie Actions (MSCA) Postdoctoral Fellowship Guarantee Funding (Ref: 101151868), which enabled her to complete this paper during her fellowship.

References

- International Energy Agency, I. (n.d.). The Future of Cooling Opportunities for energy-efficient air conditioning Together Secure Sustainable. www.iea.org/t&c/
- Ayadi, O., & Al-Dahidi, S. (2019). Comparison of solar thermal and solar electric space heating and cooling systems for buildings in different climatic regions. *Solar Energy*, 188, 545–560. https://doi.org/10.1016/j.solener.2019.06.033
- Behzadi, A., Arabkoohsar, A., Sadi, M., & Chakravarty, K. H. (2021). A novel hybrid solar-biomass design for green off-grid cold production, techno-economic analysis and optimization. *Solar Energy*, 218, 639–651. https://doi.org/10.1016/j.solener.2021.02.065
- El-Bahloul, A. A. M., Ali, A. H. H., & Ookawara, S. (2015). Performance and Sizing of Solar Driven dc Motor Vapor Compression Refrigerator with Thermal Storage in Hot Arid Remote Areas. *Energy Procedia*, 70, 634–643. https://doi.org/10.1016/j.egypro.2015.02.171
- Gao, Y., Ji, J., Guo, Z., & Su, P. (2018). Comparison of the solar PV cooling system and other cooling systems. International Journal of Low-Carbon Technologies, 13(4), 353–363. https://doi.org/10.1093/ijlct/cty035
- Gao, Y., Ji, J., Han, K., & Zhang, F. (2021). Comparative analysis on performance of PV direct-driven refrigeration system under two control methods. *International Journal of Refrigeration*, 127, 21–33. https://doi.org/10.1016/j.ijrefrig.2021.03.003
- Han, K., Ji, J., Cai, J., Gao, Y., Zhang, F., Uddin, M. M., & Song, Z. (2021). Experimental and numerical investigation on a novel photovoltaic direct-driven ice storage air-conditioning system. *Renewable Energy*, 172, 514–528. https://doi.org/10.1016/j.renene.2021.03.053
- Khalid, W., Zaki, S. A., Rijal, H. B., & Yakub, F. (2019). Investigation of comfort temperature and thermal adaptation for patients and visitors in Malaysian hospitals. *Energy and Buildings*, 183, 484–499. https://doi.org/10.1016/j.enbuild.2018.11.019
- Liang, J., Du, W., Wang, D., Yuan, X., Liu, M., & Niu, K. (2022). Analysis of the Refrigeration Performance of the Refrigerated Warehouse with Ice Thermal Energy Storage Driven Directly by Variable Photovoltaic Capacity. *International Journal of Photoenergy*, 2022. https://doi.org/10.1155/2022/3441926
- Louvet, Y. (n.d.). Heat Cost Calculations Applied to Solar Thermal Systems LCoH Calculation Method.
- Varvagiannis, E., Charalampidis, A., Zsembinszki, G., Karellas, S., & Cabeza, L. F. (2021). Energy assessment based on semi-dynamic modelling of a photovoltaic driven vapour compression chiller using phase change materials for cold energy storage. *Renewable Energy*, 163, 198–212. https://doi.org/10.1016/j.renene.2020.08.034
- Xu, Y., & Li, M. (2022). Impact of instantaneous solar irradiance on refrigeration characteristics of household PCM storage air conditioning directly driven by distributed photovoltaic energy. *Energy Science and Engineering*, 10(3), 752–771. https://doi.org/10.1002/ese3.1050
- Xu, Y., Ma, X., Hassanien, R. H. E., Luo, X., Li, G., & Li, M. (2017). Performance analysis of static ice refrigeration air conditioning system driven by household distributed photovoltaic energy system. Solar Energy, 158, 147–160. https://doi.org/10.1016/j.solener.2017.09.002